Interannual rainfall variability in the tropical Atlantic region

Guojun Gu
Goddard Earth Sciences and Technology Center, University of Maryland Baltimore County, Baltimore, Maryland, USA
Laboratory for Atmospheres, NASA Goddard Space Flight Center, Greenbelt, Maryland, USA

Robert F. Adler
Laboratory for Atmospheres, NASA Goddard Space Flight Center, Greenbelt, Maryland, USA

Received 4 March 2005; revised 26 September 2005; accepted 20 October 2005; published 19 January 2006.

[1] Rainfall variability on seasonal and interannual-to-interdecadal timescales in the tropical Atlantic is quantified using a 25-year (1979–2003) monthly rainfall data set from the Global Precipitation Climatology Project. The Intertropical Convergence Zone (ITCZ), measured by monthly rainfall between 15° and 37.5°W, attains its peak as it moves to the northernmost latitude (∼8°–10°N) during July–September, during which the most total rainfall is observed in the tropical Atlantic basin (17.5°S to 22.5°N, 15°–37.5°W); the ITCZ becomes weakest during January–February, with the least total rainfall observed as it moves to the south. In contrast, rainfall variability on interannual-to-interdecadal timescales shows a quite different seasonal preference. The most intense interannual variability occurs during March–May, when the ITCZ tends to be near the equator and becomes weaker. The relationships between rainfall anomalies in the tropical Atlantic and three distinct sea surface temperature (SST) modes are further explored on interannual-to-interdecadal timescales. The ITCZ strength and total rainfall amount in the tropical Atlantic basin are significantly modulated by the Pacific El Niño and the Atlantic equatorial mode (or Atlantic Niño) particularly during boreal spring and summer, whereas the impact of the Atlantic interhemispheric mode is considerably weaker. Regarding the anomalous latitudes of the ITCZ, the influence could come from both local, i.e., the Atlantic interhemispheric and equatorial modes, and remote forcings, i.e., El Niño; however, a direct impact of El Niño on the latitudes of the ITCZ can only be found during April–July, not in winter and early spring, during which the largest SST anomalies are usually observed in the equatorial Pacific.

Citation: Gu, G., and R. F. Adler (2006), Interannual rainfall variability in the tropical Atlantic region, *J. Geophys. Res.*, *111*, D02106, doi:10.1029/2005JD005944.

1. Introduction

[2] Tropical convection and rainfall in the Atlantic basin exhibit intense variations on various timescales [e.g., *Nobre and Shukla*, 1996; *Giannini et al.*, 2001a, 2001b; *Chiang et al.*, 2000, 2002]. A narrow band of deep convection and rainfall manifesting the Atlantic Intertropical Convergence Zone (ITCZ) is usually observed north of the equator with the northeasterly and southeasterly trade winds converging into it. This narrow band of rainfall or the ITCZ appears primarily over the open ocean, but extends to the northeast coast of tropical South America during boreal spring and to the West African continent in boreal summer, roughly following seasonal movement of warm sea surface temperature (SST) (≥27°C) (Figure 1). Fluctuations in the ITCZ's intensity and location may thus be closely connected to rainfall variability both in the tropical Atlantic basin and over the two neighboring continents [e.g., *Lamb*, 1978a, 1978b; *Nobre and Shukla*, 1996; *Grist and Nicholson*, 2001; *Biasutti et al.*, 2004]. Exploring the ITCZ variability can hence provide a reasonable and feasible perspective to Atlantic climate variability regarding the ITCZ-associated convection and rainfall and atmospheric circulation anomalies.

[3] Previous studies showed a close link between the anomalies in the strength and latitude of the Atlantic ITCZ and SST anomalies in the both equatorial Pacific and Atlantic [e.g., *Hastenrath and Greischar*, 1993; *Nobre and Shukla*, 1996; *Uvo et al.*, 1998; *Giannini et al.*, 2001b]. Two anomalous SST patterns in the tropical Atlantic are considered to be major local forcings on interannual-to-interdecadal timescales [e.g., *Carton and Huang*, 1994; *Enfield et al.*, 1999; *Servain et al.*, 1999]. The first is similar to, but much weaker than the Pacific El Niño, occurring near the equator and peaking primarily during boreal

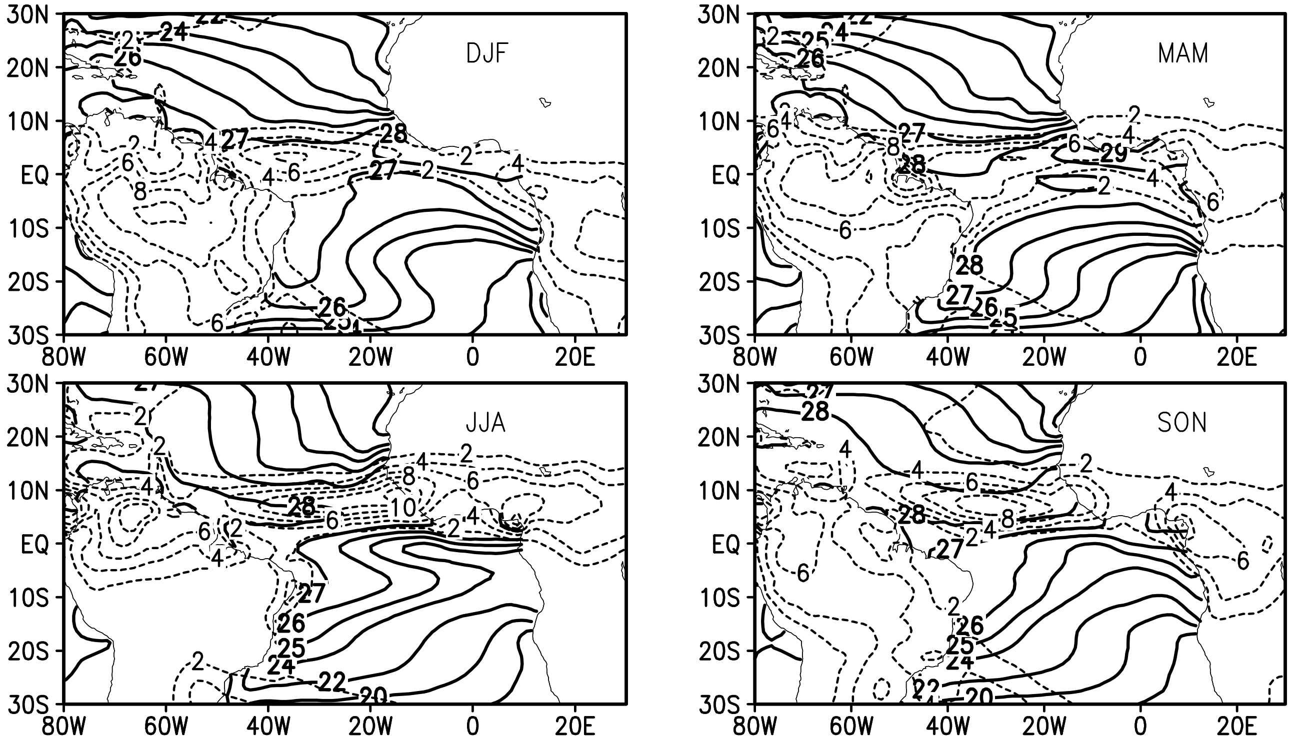

Figure 1. Seasonal mean precipitation (mm d^{-1}) and SST (°C) in the tropical Atlantic region.

summer [e.g., *Zebiak*, 1993; *Carton and Huang*, 1994; *Ruiz-Barradas et al.*, 2000]. A southward shift of convection and rainfall occurs during the warm phase of the event with evident atmospheric circulation anomalies [e.g., *Ruiz-Barradas et al.*, 2000; *Wang*, 2002], e.g., weaker trade winds in the tropical western Atlantic, and a weakened Atlantic Walker cell but a strengthened local Hadley cell. This SST anomaly feature is usually named the Atlantic equatorial mode or the Atlantic Niño despite that it is a damped mode unlike the Pacific El Niño [*Zebiak*, 1993], and may itself be strongly modulated by the equatorial Pacific [e.g., *Delecluse et al.*, 1994; *Latif and Grötzner*, 2000]. The second SST anomaly pattern is characterized as an out-of-phase SST anomaly between two regions: one is the tropical North Atlantic (5°–25°N) and the other is the tropical South Atlantic (5°–25°S). This out-of-phase SST anomaly is manifested as a cross-equatorial SST gradient reaching its maximum in boreal spring and extending to early boreal summer [e.g., *Hastenrath and Greischar*, 1993; *Nobre and Shukla*, 1996; *Sutton et al.*, 2000], though causal relations within this dipole-like phenomenon have been statistically challenged [e.g., *Houghton and Tourre*, 1992; *Enfield et al.*, 1999]. As a dominant interdecadal oscillation in the tropical Atlantic [e.g., *Ruiz-Barradas et al.*, 2000], this SST gradient mode might effectively impact the migration of the Atlantic ITCZ [e.g., *Nobre and Shukla*, 1996]. Anomalously warm (cold) north/cold (warm) south SST configuration could induce an anomalous northward (southward) shift of the ITCZ and then cause drought (flood) in the northeast part of South America [e.g., *Wagner*, 1996].

[4] In addition to the local SST modes, two other remote forcings have also been recognized [e.g., *Deque and Servain*, 1989; *Curtis and Hastenrath*, 1995; *Enfield and Mayer*, 1997; *Xie and Tanimoto*, 1998]: (1) The North Atlantic Oscillation (NAO) and related atmospheric circulation anomalies in the higher latitudes had shown impact on the tropical Atlantic by means of modulating the surface wind field and then SST [e.g., *Deque and Servain*, 1989; *Xie and Tanimoto*, 1998; *Czaja et al.*, 2002; *Wang*, 2002], while this impact is not consistently confirmed by other studies [e.g., *Ruiz-Barradas et al.*, 2000]. (2) The Pacific El Niño event can influence the Atlantic ITCZ and SST in the tropical North Atlantic [e.g., *Curtis and Hastenrath*, 1995; *Enfield and Mayer*, 1997; *Ruiz-Barradas et al.*, 2000]. Two distinct mechanisms have been proposed [e.g., *Chiang et al.*, 2002]. One is the Pacific-North-American atmospheric teleconnection (PNA) passing through the midlatitudes [e.g., *Nobre and Shukla*, 1996]. Anomalous SST warming often appears in the tropical North Atlantic about one season after the peak month of El Niño, likely caused by weakening trade winds. The other is the anomalous Walker circulation forced directly by diabatic heating anomalies in the equatorial Pacific [e.g., *Saravanan and Chang*, 2000; *Chiang et al.*, 2002]. Anomalous warm (cold) tropospheric temperatures following the warm (cold) ENSO spread across the tropical troposphere, tending to stabilize (disturb) the atmosphere and hence suppress (enhance) convection and precipitation in the tropical Atlantic [e.g., *Chiang et al.*, 2002; *Chiang and Sobel*, 2002; *Giannini et al.*, 2004].

[5] *Chiang et al.* [2002] mentioned both mechanisms related to El Niño, and showed that a strong anomalous Walker cell during the El Niño causes negative rainfall anomalies in the tropical Atlantic. Local SST gradient mode was also discussed in their study. An anomalous warm north/cool south SST pattern manifesting a strong northward SST gradient effectively shifts the Atlantic ITCZ to the north. The physical pictures associated with these changes were further explored by documenting the ITCZ

variability's seasonal dependence, sensitivity to small anomalous SST gradients, and possible modulations of SST anomalies. The most interesting part in their work is that they are primarily concentrated on the variations of the Atlantic ITCZ represented by monthly precipitation, not as most previous studies which focused on SST anomalies [e.g., *Curtis and Hastenrath*, 1995; *Nobre and Shukla*, 1996; *Sutton et al.*, 2000].

[6] *Chiang et al.* [2002], however, did not discuss the role of Atlantic equatorial mode in the ITCZ variability. They primarily focused on boreal spring in which the most intense interannual-to-interdecadal variability is usually found. The Atlantic equatorial mode usually becomes active during boreal late spring and summer, and modulates convection and precipitation in the equatorial region [e.g., *Sutton et al.*, 2000; *Ruiz-Barradas et al.*, 2000]. Intense tropical weather and rainfall systems, such as African easterly waves and tropical cyclones, frequently appear along the Atlantic ITCZ during boreal summer. These systems have shown evident interannual variability [e.g., *Thorncroft and Rowell*, 1998; *Landsea et al.*, 1999; *Gu et al.*, 2003]. Hence quantifying rainfall variability, especially the ITCZ variability during boreal summer and fall, may provide some clues to understanding these variabilities, specifically the variability in West African monsoon system and Atlantic hurricane activity [e.g., *Lamb*, 1978a, 1978b; *Janicot et al.*, 1998; *Landsea et al.*, 1999].

[7] Therefore, instead of only focusing on boreal spring, rainfall variability in all seasons will be investigated here. We focus our attention on interannual rainfall variability in the tropical Atlantic and particularly the Atlantic ITCZ-related variability. Seasonal dependence will be explored according to the dominant local and remote SST forcing modes. Our objectives are (1) to document the correlations between rainfall and SST modes, (2) to investigate the seasonal dependence of rainfall variability, and (3) hence to explore physical mechanisms that may explain major features of the Atlantic ITCZ on interannual-to-interdecadal timescales.

[8] The data sets used in this study are introduced in section 2. Seasonal rainfall variation in the tropical Atlantic is described in section 3. Rainfall variability on the interannual timescale is then quantified with a specific focus on the Atlantic ITCZ represented by monthly precipitation. The relationships between rainfall and SST anomalies are investigated in section 4. Summary and discussions are given in section 5.

2. Data

[9] A 25-year (1979–2003) monthly mean rainfall data set from the Global Precipitation Climatology Project (GPCP) is used to quantify the Atlantic ITCZ and rainfall variability. On a global $2.5^\circ \times 2.5^\circ$ grid, the data is combined from various information sources [*Adler et al.*, 2003]: the infrared (IR) rainfall estimates from geostationary and polar-orbiting satellites, the microwave estimates from Special Sensor Microwave/Imager (SSM/I), and surface rain gauges from the Global Precipitation Climatological Centre (GPCC).

[10] The SST anomalies and related SST modes in both tropical Atlantic and Pacific Oceans are estimated using a 22-year (1982–2003) monthly mean SST data set [*Reynolds and Smith*, 1994]. This data set is produced using both in situ and satellite observations, and archived on $1^\circ \times 1^\circ$ grids.

3. Variability and Structure of Rainfall Anomalies

3.1. Seasonal Variation

[11] Seasonal mean rainfall in the tropical Atlantic basin and neighboring continents is shown in Figure 1 together with seasonal mean SST. A narrow band of rainfall over the open ocean manifesting the marine ITCZ can be seen year-round, roughly over the regions with higher SST ($\geq 27^\circ$C). During boreal winter and spring, the marine ITCZ is weaker and located near the equator. It becomes much stronger in boreal summer and fall as it moves away from the equator to reach its northernmost position, concomitant with the occurrence of an equatorial cold tongue. Interestingly, the warmest SSTs, however, occur during March–May. Particularly, the warm SSTs ($\geq 29^\circ$C) in the eastern Atlantic basin (east of about 10°W) during this period correspond to the peak rainfall season near the Gulf of Guinea during May to June [e.g., *Mitchell and Wallace*, 1992; *Gu and Adler*, 2004].

[12] Seasonal rainfall variations are evident over land. Convection and rainfall over West Africa (west of about 10°E) show a quite similar seasonal cycle as the marine ITCZ. No significant rainfall occurs during boreal winter, though a weak rainy zone is located in the tropical eastern Atlantic connecting the marine ITCZ and a large area of rainfall over the southern part of the African continent. Convection and rainfall over West Africa peak in boreal summer. A similar seasonal cycle existing in rainfall over West Africa as in the marine ITCZ probably suggests a strong seasonal modulation by SST in the tropical Atlantic [e.g., *Biasutti et al.*, 2004]. Using recently archived satellite observations, *Gu and Adler* [2004] detailed the seasonal evolution pattern of the entire coupled system in the tropical eastern Atlantic and West Africa, and emphasized the influence of SST and its related dynamic forcing on seasonal rainfall variability near the Gulf of Guinea.

[13] Convection and rainfall over the tropical South America, however, exhibit a quite different seasonal evolution pattern likely because of distinct geographical configurations. Most intense convection and rainfall appear during boreal winter, covering a large area of land mostly south of the equator; in contrast, the marine ITCZ is rarely south of the equator; the major rainfall area over land gradually moves to the north roughly following the seasonal march of insolation on the Earth [e.g., *Biasutti et al.*, 2004]; convection and rainfall become weaker in boreal summer and fall as the major rainy zone approaches and crosses the equator; in particular, a narrow east-west band structure of rainfall cannot consistently be observed, showing a rainfall pattern distinct from the marine ITCZ. Thus the seasonal march of rainfall over South America might primarily be controlled by insolation as expected, whereas oceanic impact may become important only during boreal spring when the marine ITCZ moves close to the equator and becomes more connected with convection over land. *Biasutti et al.* [2003, 2004] explored and compared various physical mechanisms

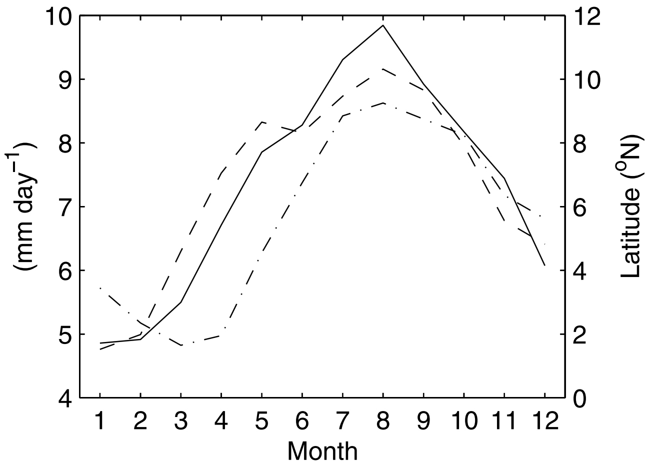

Figure 2. Seasonal mean precipitation in the center of the Atlantic ITCZ (mm d^{-1}; solid line) and averaged over 17.5°S to 22.5°N, 15°–37.5°W (0.3 × mm d^{-1}; dashed line), and seasonal mean latitudes of the center of the Atlantic ITCZ (°N; dash-dotted line).

related to the annual variations of both the marine ITCZ and land precipitation through analyzing the outputs of an atmospheric GCM.

[14] To limit the effects of continents, here we primarily focus on the marine ITCZ defined by monthly mean rainfall between 15°W and 37.5°W, though the possible impact of convection over land on the marine ITCZ may still exist [*Biasutti et al.*, 2004]. The position and strength of the ITCZ are represented by the latitude and magnitude of maximum precipitation, respectively. The basin-mean rainfall (17.5°S to 22.5°N, 15°–37.5°W) is further calculated to assess total rainfall variability in the tropical Atlantic basin and as a comparison with the ITCZ strength. The 25-year mean seasonal cycles are then estimated for these three quantities (Figure 2). Compared to Figure 1, Figure 2 illustrates a more quantitative description of seasonal variations in the tropical Atlantic. The ITCZ attains its southernmost (northernmost) position during March–April (July–August). Rainfall intensity represented by both the ITCZ strength (solid line in Figure 2) and basin-mean rainfall (dashed line in Figure 2) peaks in August, and becomes weakest during January–February. It is interesting to note that the ITCZ strength and basin-mean rainfall generally follow each other, though there is a second peak in May for the latter probably due to a relatively scattered structure of the ITCZ during this time period, particularly in the western portion of the tropical Atlantic where there often appears a southern branch of the ITCZ (Figure 1) [*Liu and Xie*, 2002; *Grodsky and Carton*, 2003].

3.2. Interannual-to-Interdecadal Variability

[15] Seasonal mean interannual variances of rainfall and SST are shown in Figure 3. Most intense variances of precipitation are observed during boreal winter and spring, tending to be located in the western basin and over the northeast coastal region of South America. During boreal summer, the maximum variance zone moves to the north following the movement of the ITCZ, but becomes relatively weaker than in the earlier seasons. The smallest rainfall variances are observed during boreal fall. This seasonal evolution pattern is basically consistent with past discoveries [e.g., *Hastenrath and Greischar*, 1993; *Nobre*

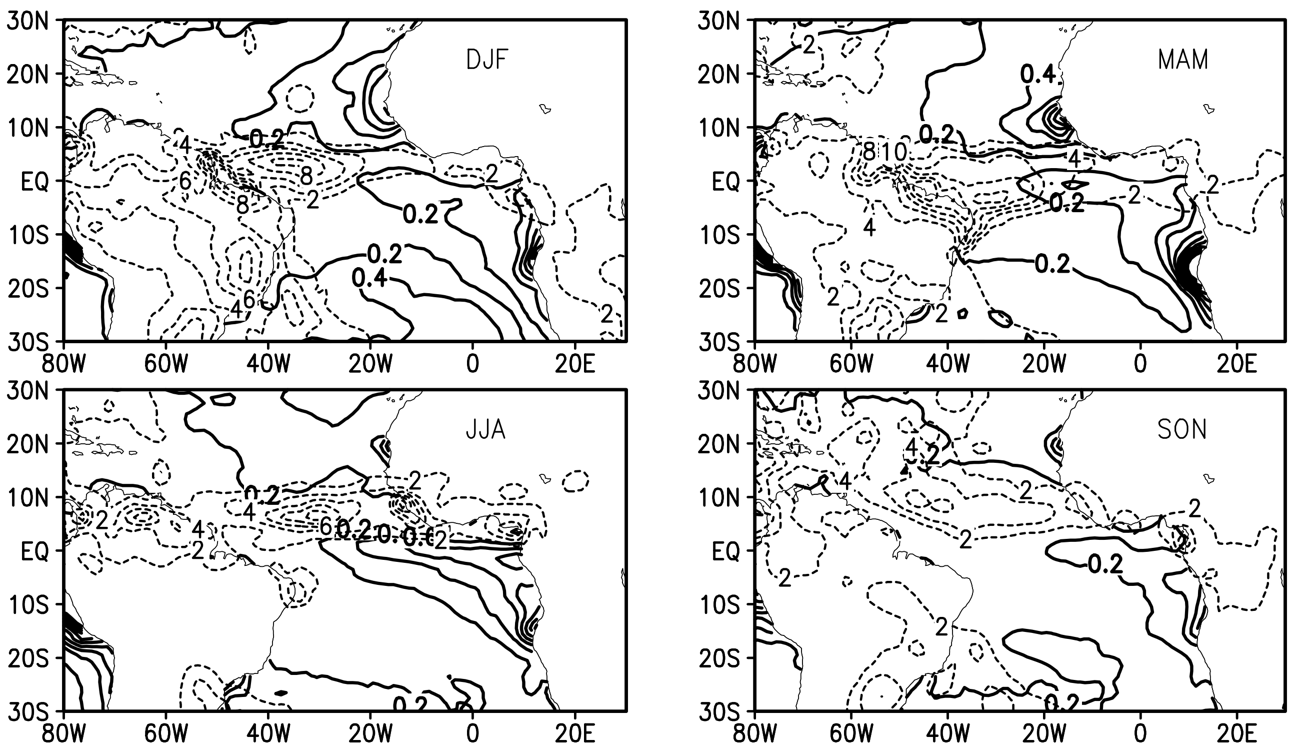

Figure 3. Seasonal mean variances of precipitation (mm^2 d^{-2}) and SST ((°C)^2) in the tropical Atlantic region.

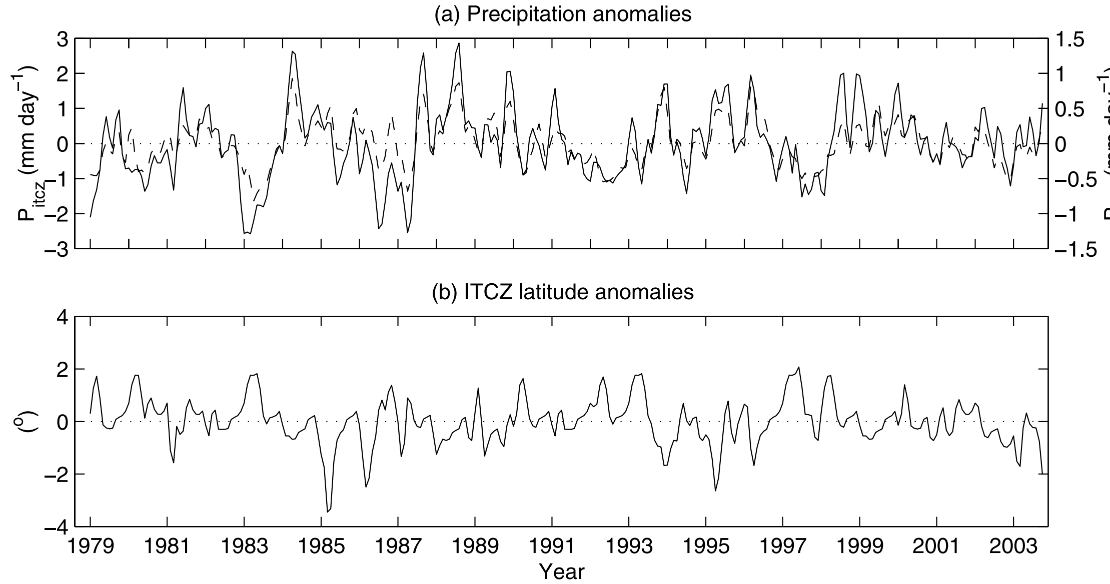

Figure 4. (a) Precipitation anomalies (mm d^{-1}) in the center of the Atlantic ITCZ (P_{itcz}; solid line) and over 17.5°S to 22.5°N, 15°–37.5°W (P_{dm}; dashed line). (b) Anomalies (degrees) of the central latitudes of the Atlantic ITCZ. The Atlantic ITCZ is defined between 15°W and 37.5°W. Shown here are three-month running averages.

and Shukla, 1996]. Compared to rainfall variances, SST variances tend to be located in the eastern portion of the basin. Furthermore, during boreal winter and spring, no strong variances can be observed near the equator. Evident equatorial SST variances can only be observed during boreal summer, probably corresponding to the anomalous warm/cold events occurring every 2–4 years [e.g., *Zebiak*, 1993]. SST variances seem to be a passive response to atmospheric anomalies mostly originating in the western basin. However, the modulations of rainfall variability by SST anomalies can also be deduced. For instance, intense rainfall variances near the Gulf of Guinea during June–August are probably reflecting SST modulations associated with the Atlantic equatorial mode [*Ruiz-Barradas et al.*, 2000].

[16] To further explore rainfall variability on interannual and/or longer timescales, three anomaly time series corresponding to the ITCZ strength (solid line in Figure 4a), the ITCZ position (Figure 4b), and the basin-mean rainfall (dashed line in Figure 4a) are constructed by subtracting their respective mean seasonal cycles, and denoted as P_{itcz}, LAT_{itcz}, and P_{dm}, respectively (Figure 4).

[17] Domain-mean variance of rainfall anomalies (PT_{atl}) in the tropical Atlantic (17.5°S to 22.5°N, 15°–37.5°W), and variances of P_{itcz} and LAT_{itcz} are further depicted in Figure 5 as a function of month. As in Figure 3, evident seasonal dependence is shown, particularly in variances of PT_{atl} and LAT_{itcz}. For them, the largest (smallest) variances occur during boreal spring (fall) [e.g., *Chiang et al.*, 2002]. However, the variance of P_{itcz} shows a complicated and different seasonal preference. In addition to a peak in April, two other ones occur during January and July–August, respectively. This may imply that during these months some large-scale modes come to modulate the ITCZ intensity, but cannot effectively influence total rainfall amount and the ITCZ locations. More discussions will be given in next section.

[18] *Chiang et al.* [2002] discussed interdependence between the ITCZ strength and position. The two are significantly, negatively correlated in several months, i.e., January, April, May and July. More (less) rainfall appears as the ITCZ stays farther south (north), quite different from the ITCZ variability on the seasonal timescale (Figures 1 and 2). Because of the strong seasonal dependence of interannual-to-interdecadal variances (Figure 5) and a different data set used here than that used by *Chiang et al.*

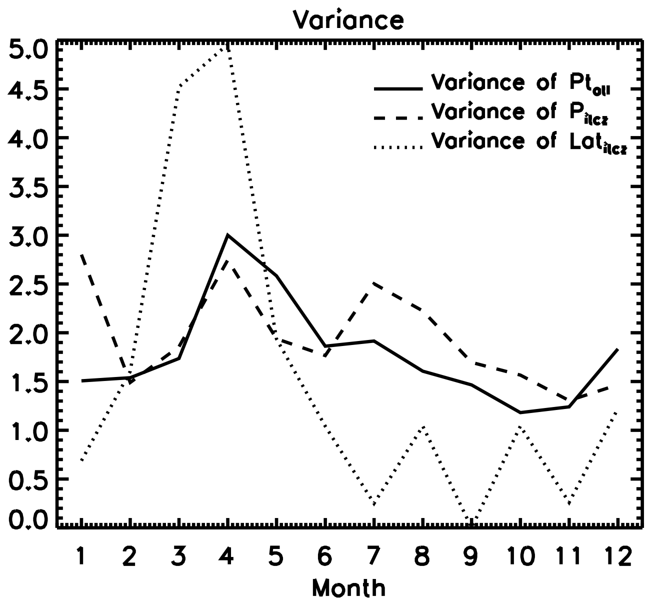

Figure 5. Mean variance of precipitation anomalies over 17.5°S to 22.5°N, 15°–37.5°W (solid line); variance of precipitation anomalies in the center of the Atlantic ITCZ (dashed line) and latitudinal anomalies of the Atlantic ITCZ (dotted line) as a function of month.

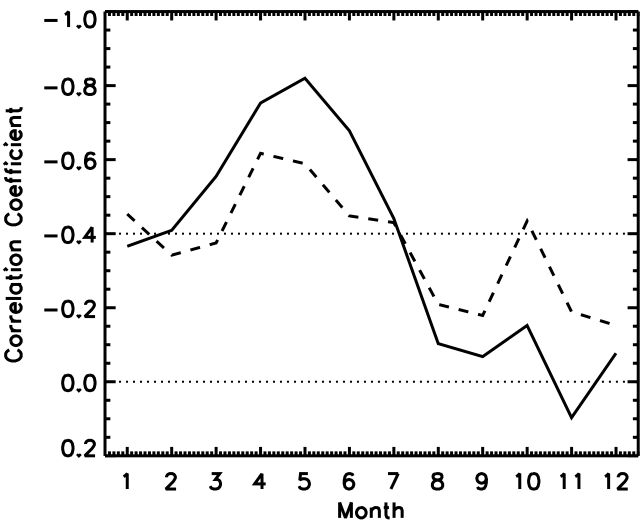

Figure 6. Linear correlation between the precipitation anomalies averaged over 17.5°S to 22.5°N, 15°–37.5°W (P_{dm} (mm d^{-1}); solid line), and in the center of the Atlantic ITCZ (P_{itcz} (mm d^{-1}); dashed line), and the Atlantic ITCZ's latitudinal anomalies (LAT_{itcz}). $\gamma = \pm 0.4$ denotes the 5% confidence level based on 23 degrees of freedom.

[2002], linear correlations between P_{itcz} and LAT_{itcz} (dashed line in Figure 6), and between P_{dm} and LAT_{itcz} (solid line in Figure 6) are calculated. As expected, significantly negative correlations between P_{itcz} and LAT_{itcz} appear during boreal spring. Different from *Chiang et al.* [2002], significant correlations can also be seen in July and October. We call this relation between the ITCZ's strength and latitudinal location its self-correlation. Furthermore, a stronger and more consistent interdependence can be found between P_{dm} and LAT_{itcz}. The correlation coefficients between these two parameters are above the 5% confidence level from February to July, which might suggest that anomalous positions of the ITCZ are more associated with the basin-mean rainfall anomalies than the ITCZ's strength due to its somewhat scattered structure in these months [*Liu and Xie*, 2002; *Grodsky and Carton*, 2003].

4. Relationships Between Rainfall and SST Anomalies

[19] Three SST anomaly time series are constructed to represent the three known SST modes: the Pacific El Niño (NINO3) (solid line in Figure 7a), Atlantic Niño (ATL3) (dashed line in Figure 7a), and Atlantic interhemispheric mode (TNA-TSA) (Figure 7b). These three modes are generally considered to be the major, somewhat competing factors modulating climate variability in the tropical Atlantic [e.g., *Servain et al.*, 1999; *Ruiz-Barradas et al.*, 2000; *Wang*, 2002]. NINO3 and ATL3 are defined as the mean SST anomalies within the domains of 5°S to 5°N, 90°–150°W, and 4°S to 4°N, 0° to 20°W, respectively; TNA-TSA is denoted as the difference of SST anomalies between two domains in the tropical Atlantic, i.e., 5°–25°N, 16°–56°W (tropical North Atlantic), and 5°–25°S, 30°W to 10°E (tropical South Atlantic). TNA (TSA) represents the domain-mean SST anomalies in the tropical North (South) Atlantic.

4.1. Seasonal Correlations Between SST Indices

[20] Weak correlation between NINO3 and ATL3 has been shown in past studies [e.g., *Ruiz-Barradas et al.*, 2000; *Wang*, 2002]. Regarding strong seasonal dependence (not shown) [e.g., *Wang*, 2002], we examine the impact of El Niño on ATL3 by means of estimating correlation

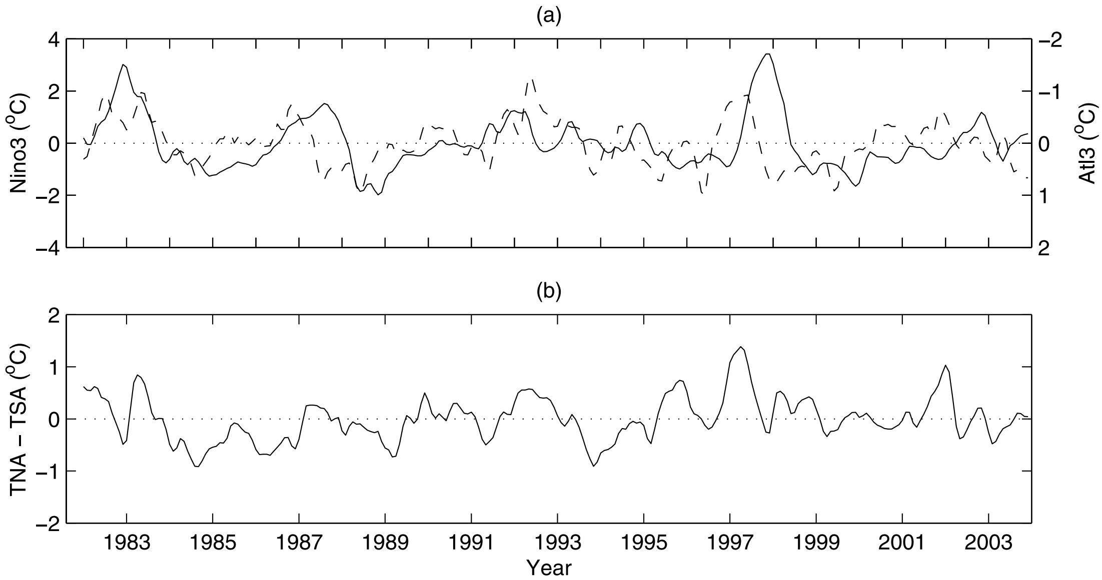

Figure 7. (a) SST anomalies (°C) represent the eastern Pacific Niño 3 mode (NINO3 (5°S to 5°N, 90°–150°W); solid line) and the Atlantic equatorial mode (ATL3 (4°S to 4°N, 0°–20°W); dashed line); (b) SST anomaly difference (°C) between the tropical North and South Atlantic oceans (TNA-TSA) represents the interhemispheric gradient mode. TNA and TSA represent the domains of 5°–25°N, 16°–56°W, and 5°–25°S, 30°W to 10°E, respectively. Three-month running average is applied.

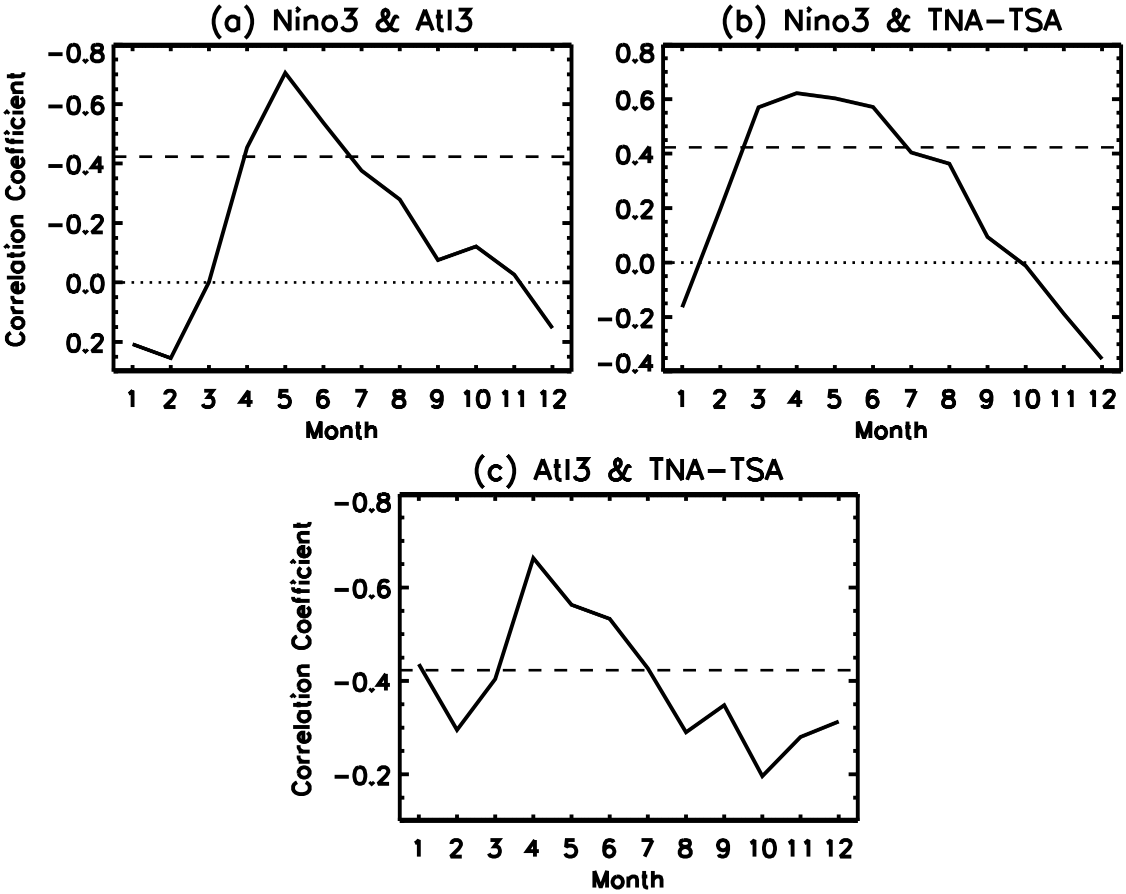

Figure 8. Linear correlation between (a) NINO3 and ATL3, (b) NINO3 and TNA-TSA, and (c) ATL3 and TNA-TSA. Dashed lines denote the 5% confidence level based on 20 degrees of freedom.

coefficients at each individual month (Figure 8a), rather than computing the coefficients between the entire time series. Significant correlations between them can be found during April–June, suggesting possible external modulation of the Atlantic equatorial mode during this season [e.g., *Delecluse et al.*, 1994; *Latif and Grötzner*, 2000].

[21] The interhemispheric mode (TNA-TSA) usually peaks during boreal spring and early summer (not shown). A strong lag correlation between TNA-TSA and the El Niños via PNA has already been shown in previous studies [e.g., *Lanzante*, 1996; *Enfield and Mayer*, 1997]. TNA-TSA during March–May is significantly correlated with NINO3 during the prior December–February (Table 1). Interestingly, the contemporaneous correlation between them during March–May is even stronger. However, TNA shows a stronger lag correlation with NINO3, consistent with past conclusions [e.g., *Curtis and Hastenrath*, 1995; *Lanzante*, 1996]. Significantly negative, contemporaneous correlation between TSA and NINO3 can also be found during March–May, generally consistent with the composite analyses given by *Chiang et al.* [2002], but quite different from other past studies [e.g., *Enfield and Mayer*, 1997]. Furthermore, it seems that the impact of El Niño on the tropical South Atlantic does not go through PNA since the correlation between TSA_{MAM} and $NINO3_{DJF}$ is very weak (Table 1). Contemporaneous correlation between NINO3 and TNA-TSA is further computed as a function of month (Figure 8b). Significant correlation between them can be seen during March–June, further implying that the ENSO events may directly influence either component of TNA-TSA via anomalous Walker circulation, in addition to their remote modulation of TNA through the midlatitudes.

[22] Within the tropical Atlantic, ATL3 and TNA-TSA are significantly correlated in January and during April–July (Figure 8c), roughly in agreement with past studies [e.g., *Servain et al.*, 1999]. This relationship is reasonable because ATL3 represents part of the variability in the tropical South Atlantic (strong correlation can readily be found between ATL3 and TSA (not shown)), despite the fact that the maximum variances of these two appear in

Table 1. Correlations γ of NINO3 During December-January-February and the Following March-April-May With TNA, TSA, and TNA-TSA During the Following March-April-May[a]

	γ		
	TNA_{MAM}	TSA_{MAM}	$TNA\text{-}TSA_{MAM}$
$NINO3_{DJF}$	**0.63**	−0.03	**0.47**
$NINO3_{MAM}$	**0.53**	**−0.42**	**0.69**

[a]Here, γ = 0.42 is the 5% confidence level based on 20 degrees of freedom. DJF, December-January-February; MAM, March-April-May.

Table 2. Correlation Coefficients γ Between the Precipitation Anomalies Averaged Over 17.5°S to 22.5°N, 15°–37.5°W, and in the Center of the Atlantic ITCZ, the Anomalies of the Central Latitudes of the Atlantic ITCZ, and the Time Series of SST Anomalies Representing Various Tropical Oscillation Modes[a]

	γ				
	NINO3	ATL3	TNA-TSA	TNA	TSA
P_{dm}	**−0.53**	**0.53**	−0.33	−0.05	0.38
P_{itcz}	**−0.49**	**0.5**	−0.15	0.08	0.28
LAT_{itcz}	0.3	**−0.47**	**0.5**	0.24	−0.41

[a]Here, γ = 0.42 is the 5% confidence level based on 20 degrees of freedom. P_{dm}, precipitation anomalies averaged over 17.5°S to 22.5°N, 15°–37.5°W (mm d^{-1}); P_{itcz}, precipitation anomalies in the center of the Atlantic ITCZ (mm d^{-1}), LAT_{itcz}, anomalies of the central latitudes of the Atlantic ITCZ (degrees).

different seasons, that is, during May–July and January–May, respectively (not shown).

4.2. Correlations of SST Indices With Rainfall Anomalies and the ITCZ

[23] Contemporaneous linear correlations between rainfall time series and SST indices are computed (Table 2). Both ENSO (NINO3) and the Atlantic equatorial mode (ATL3) show significant impact on rainfall anomalies in the tropical Atlantic region, though the signs of their impact are always opposite. The warm (cold) events in the tropical central eastern Pacific tend to suppress (enhance) rainfall in the tropical Atlantic [e.g., *Saravanan and Chang*, 2000; *Giannini et al.*, 2001b; *Chiang et al.*, 2002]; in contrast, the warm (cold) phase of the Atlantic equatorial mode tends to enhance (decrease) rainfall in the basin. Furthermore, the Atlantic equatorial mode seems to influence the latitudes of the Atlantic ITCZ. Warmer (colder) SST in the deep tropics tends to move the ITCZ southward (northward). This mode can thus be one of the important factors modulating summer rainfall variability over West Africa [e.g., *Janicot et al.*, 1998], particularly near the Gulf of Guinea. However, the correlation between NINO3 and LAT_{itcz} is not statistically significant, showing a much weaker simultaneous impact of ENSO, inasmuch as it could still influence the latitudes of the ITCZ via another means by modulating the tropical North Atlantic SST (Table 1) [e.g., *Curtis and Hastenrath*, 1995; *Nobre and Shukla*, 1996]. In addition, ATL3 and NINO3 are significantly, negatively correlated during April–June (Figure 8a), forming a much more complicated pattern.

[24] SST anomalies in either north or south tropical Atlantic are not significantly correlated to rainfall and ITCZ indices. However, their difference (TNA-TSA) representing the Atlantic interhemispheric mode significantly correlates with LAT_{itcz}, suggesting strong impact on the positions of the ITCZ. Anomalous latitudes of the ITCZ during boreal spring are closely related to anomalous rainfall patterns in northeast Brazil [e.g., *Nobre and Shukla*, 1996]. Nevertheless, TNA-TSA shows much weaker correlation with either P_{dm} or P_{itcz}, implying a limited direct forcing of rainfall anomalies by this gradient.

[25] Seasonal dependence of the relationship between SST modes and rainfall anomalies are further explored by computing correlation coefficients as a function of month (Figures 9 and 10). NINO3 is strongly correlated with both P_{itcz} and P_{dm} during January–February and April–July (Figure 9a). Particularly, during April–July the correlation between NINO3 and P_{dm} is consistently stronger than between NINO3 and P_{itcz}, indicating a widespread modulation of rainfall in the equatorial region by the tropical Pacific as suggested by past studies [e.g., *Chiang et al.*, 2002]. Significant correlations are also observed between NINO3 and LAT_{itcz} during April–July (Figure 10a). This seems to suggest seasonal modulations of the ITCZ locations by ENSO. However, we have to note that the intensity and position of the ITCZ are strongly correlated with each other during this period (Figure 6). It is thus possible that this ITCZ's self-correlation contributes a lot to the seemingly direct modulation of LAT_{itcz} by NINO3. From Figure 9a, we can also find that in March the correlation between NINO3 and rainfall anomaly indices is weak as discovered before [e.g., *Uvo et al.*, 1998; *Chiang et al.*, 2002]. Neither P_{itcz} nor P_{dm} is significantly correlated with NINO3 in March. A composite monthly evolution of the warm ENSO events indicates that this weak correlation feature in March might be caused by a competition of the ENSO's two-way impact (not shown). Warm SSTs in the tropical central eastern Pacific associated with El Niño peaking in boreal winter may immediately force intense negative rainfall anomalies in the tropical Atlantic and northeast South America via anomalous Walker circulation and tropospheric warming [e.g., *Chiang and Sobel*, 2002]. On the other hand, remote modulation of SST in the tropical North Atlantic by El Niño through midlatitudes can also be observed following the tropical Pacific warming, but probably several months later (Table 1). Consequently, warm SST gradually takes control in the tropical North Atlantic tending to enhance convection and rainfall north of the equator, while the direct impact of Pacific El Niño continues to be felt in the equatorial region. March turns out to be right in the middle of this transition originating from the equatorial Pacific.

[26] Correlations between ATL3 and P_{dm} are consistently above the 5% confidence level during April–September (solid line in Figure 9b), showing a strong impact of the Atlantic equatorial mode on rainfall variability during this period in which the warmest SST anomalies are usually observed in the equatorial region. Correlations of P_{itcz} with ATL3 are relatively weaker (dashed line in Figure 9b); the correlation coefficient becomes statistically significant only in April and during July–August. For ATL3 and LAT_{itcz}, significant correlations appear in several months: November–February and April–June (Figure 10b), implying anomalous latitudes of the ITCZ accompanying rainfall anomalies. Particularly during November–February, warm (cold) events can be seen in the equatorial Atlantic (Figure 7) [*Wang*, 2002], while they seemingly cannot effectively induce significant rainfall anomalies (Figure 9b). Composite maps of the warm events show a coherent spatial pattern (not shown): A band of positive rainfall anomalies appears across the equator in the eastern basin and cross-equatorial northwesterly to equatorial westerly wind anomalies, along with a large area of warm SST, occupy the eastern equatorial region just south of the West African continent. This coherent spatial pattern is consistent with other studies and might suggest a relatively strong dynamic

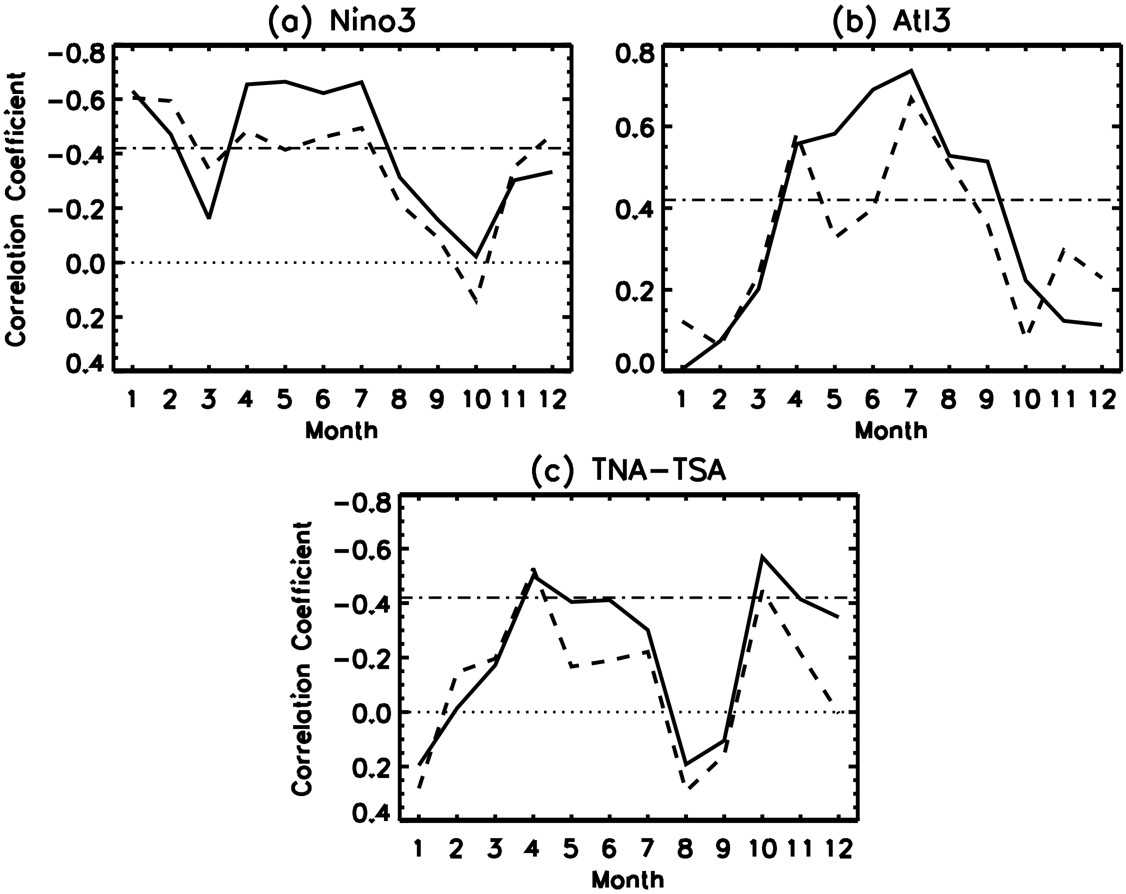

Figure 9. Linear correlation between the precipitation anomalies averaged over 17.5°S to 22.5°N, 15°–37.5°W (P_{dm} (mm d^{-1}); solid lines), and in the center of the Atlantic ITCZ (P_{itcz} (mm d^{-1}); dashed lines), and the SST anomalies (°C) representing (a) the eastern Pacific Niño 3 mode (NINO3), and the Atlantic equatorial modes: (b) ATL3 and (c) TNA-TSA. Here, $\gamma = \pm 0.42$ denotes the 5% confidence level based on 20 degrees of freedom.

coupling during the Atlantic Niños [e.g., *Zebiak*, 1993; *Ruiz-Barradas et al.*, 2000].

[27] As indicated in Table 1, only weak correlations can be found between TNA-TSA and rainfall indices, i.e., P_{itcz} and P_{dm} (Figure 9c). Correlation coefficients above the 5% confidence level appear only in two months: April and October. However, consistent, significant correlations between TNA-TSA and LAT_{itcz} are observed during boreal spring and early summer with only one exception, March (Figure 10c). The results enhance the argument that during boreal spring the Atlantic interhemispheric mode could effectively impact the latitudes of the ITCZ but have much less influence on the magnitude of rainfall anomalies in the tropical Atlantic. On the other hand, it tends to suggest that this interhemispheric mode may also play a role during boreal summer as does the Atlantic equatorial mode [e.g., *Wang*, 2002], thus making the summer variability pattern much more complicated.

5. Summary and Concluding Remarks

[28] Rainfall variability on seasonal and interannual-to-interdecadal timescales in the tropical Atlantic is quantified using the 25-year GPCP product. Evident seasonal variations exist in the basin-mean rainfall, and the marine ITCZ and its latitudes. More (less) basin-mean rainfall and a stronger (weaker) ITCZ are observed when it moves to the north (south) during boreal summer and fall (winter and spring). However, the most intense variations of rainfall on interannual-to-interdecadal timescales occur during boreal spring, showing a different seasonal preference. Also, the interannual-to-interdecadal variances of rainfall tend to be located in the western equatorial region. In contrast, major SST variances on interannual-to-interdecadal timescales prefer the eastern portion of the basin. This contrasting structure probably indicates a unique relationship between rainfall and SST on interannual-to-interdecadal timescales.

[29] Correlation analyses indicate that rainfall anomalies including the basin-mean rainfall and ITCZ intensity are strongly modulated by SST anomalies in both the tropical Pacific (NINO3) and Atlantic (ATL3). El Niños influence the tropical Atlantic through two distinct means [e.g., *Saravanan and Chang*, 2000; *Giannini et al.*, 2001b; *Chiang et al.*, 2002]: (1) modulating SST in the tropical North Atlantic through PNA several months after the tropical Pacific anomalies; and (2) suppressing rainfall in the equatorial Atlantic via an anomalous Walker circulation and increased stability through widespread tropospheric

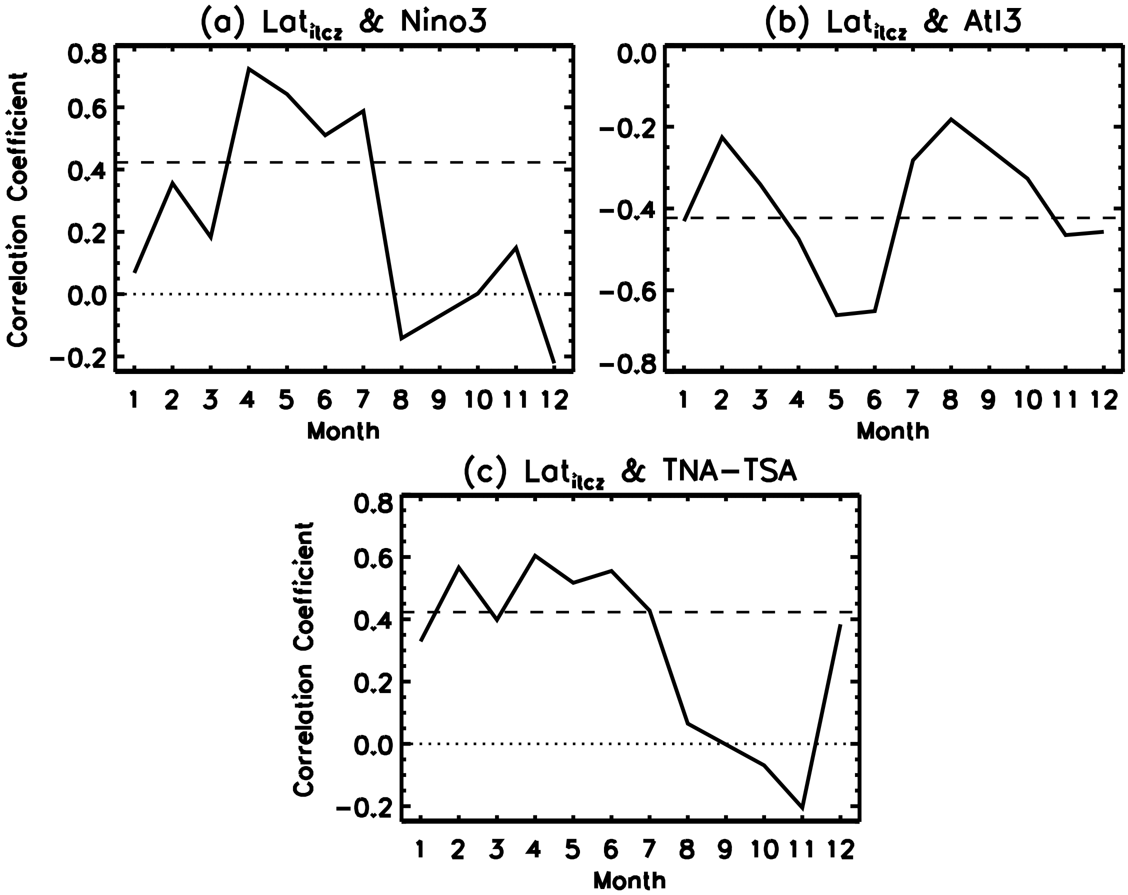

Figure 10. Linear correlation between the latitudinal anomalies of the center of the Atlantic ITCZ (LAT_{itcz}), and the SST anomalies representing (a) the eastern Pacific Niño 3 mode (NINO3), (b) the Atlantic equatorial mode (ATL3), and (c) the Atlantic gradient mode (TNA-TSA). Dashed lines denote the 5% confidence level based on 20 degrees of freedom.

warming in the tropics with a much smaller time lag. The rainfall anomalies in the western basin may be further related to surface wind anomalies, and hence probably to the SST anomalies in the equatorial and tropical South Atlantic. The time lag between these two influences is evident in the composite maps for the warm ENSO events (not shown), as are the opposite, self-competing impacts of El Niños in the tropical Atlantic. It is thus likely that because of these opposite impacts, strong negative rainfall anomalies covering the tropical Atlantic basin in January gradually evolve into a positive-negative dipole in rainfall anomalies in May. This may further explain why the correlation between rainfall anomalies and NINO3 is so weak in March (Figures 9 and 10) [*Uvo et al.*, 1998]. Also, it seems that the Pacific El Niño could significantly contribute to the Atlantic interhemispheric mode through distinct modulations of SST south and north of the equator, consistent with *Chiang et al.* [2002].

[30] Atlantic Niños can directly influence both rainfall and latitudes of the ITCZ, though it appears that the Atlantic equatorial warming itself might be externally forced [e.g., *Delecluse et al.*, 1994; *Latif and Grötzner*, 2000]. The warm events usually occur during boreal summer or late spring. A composite analysis of the peak warm months indicates a coupled, coherent spatial pattern (not shown) [e.g., *Zebiak*, 1993]. On the other hand, the Atlantic interhemispheric mode can effectively impact the locations of the ITCZ, particularly during boreal spring and early summer, but has little influence on the magnitudes of rainfall anomalies.

[31] This study provides an observational quantification of rainfall variability in the tropical Atlantic. The relationships between rainfall anomalies and (local and remote) SST forcings are also investigated. However, detailed mechanisms about these relationships are still not quite clear and straightforward possibly because of the existence of several competing forcing modes in the basin, particularly during boreal late spring and summer [e.g., *Sutton et al.*, 2000]. Further explorations of air-sea coupling processes in the tropical Atlantic and external or remote influences may be done in the future with the help of well-designed, more realistic coupled models on the basis of past results [e.g., *Chang et al.*, 2000; *Saravanan and Chang*, 2000], and also with the availability of more high-quality in situ and satellite observations. Thus several related issues have not been addressed here.

[32] 1. Anomalous warm SSTs occur in the tropical North Atlantic several months after the peaks of El Niños in the Pacific [e.g., *Chiang et al.*, 2002]. How these warm SSTs impact rainfall patterns besides their contribution to the SST gradient mode is still a puzzle in that the most intense

rainfall anomalies tend to be in the western portion of the basin.

[33] 2. El Niños may also have impact on the SSTs along and south of the equator through an indirect way partly shown in this study. For instance, intense surface wind anomalies occurring during boreal spring following El Niños and associated rainfall anomalies might be connected to SST anomalies in the eastern Atlantic basin [e.g., *Carton and Huang*, 1994; *Florenchie et al.*, 2004]. Anomalous cold SSTs are observed in both the Benguela Niño and Atlantic Niño regions one or two months after the most intense rainfall and cross-equatorial wind anomalies in the western portion of the tropical Atlantic (not shown). This seems to be in contrast with past results [e.g., *Enfield and Mayer*, 1997] and has yet to be further examined.

[34] 3. What physical mechanisms control the Atlantic equatorial anomalies during boreal summer and fall is still a question. The Pacific El Niño may excite response in the equatorial Atlantic [*Chiang et al.*, 2002]. In the tropical Atlantic, anomalously strong rainfall anomalies often occur in April prior to the equatorial warming, and high lag correlations between surface wind anomalies in the west basin and SST anomalies in the eastern basin can always be found. From 1982 to 2003, all four cold events (in 1982, 1983, 1992, and 1997) occurring in the equatorial Atlantic followed the anomalous warm events in the Pacific. Furthermore, except for 1985, the other three evident La Niñas in the Pacific are followed by Atlantic Niños. Thus it seems to suggest that Atlantic Niño might be connected to the tropical Pacific through intense modulations of ENSO on the tropical Atlantic basin during boreal spring [e.g., *Delecluse et al.*, 1994; *Latif and Grötzner*, 2000]. The Atlantic SST anomalies along the equator become strong only after May, and may thus be a time lag, remote, oceanic response to rainfall and surface wind anomalies in the western portion of the basin [e.g., *Zebiak*, 1993; *Florenchie et al.*, 2004]. However, one or two months before the peak warm month, rainfall and surface wind anomaly features could be totally different, such as in 1987 and 1988 (not shown), thus implying that the Atlantic equatorial anomalies might also be related to other factors.

[35] 4. Intense atmospheric (rainfall and surface winds) responses to the equatorial Pacific during boreal spring are evident in the western portion of the basin including the northeast coastal region of South America, suggesting a relatively easier communication can be built between remote forcing and surface through moist convection within the ITCZ [*Chiang and Sobel*, 2002]. Further examinations of the Atlantic Niño events indicate (not shown), even in the quiet years of Pacific, strong rainfall and surface wind anomalies in the west equatorial region could still be found often one or two months before the equatorial warming. Convection over land may thus be one of the major reasons as suggested by *Biasutti et al.* [2004], and their relationships with oceanic components have to be quantified in the future.

[36] 5. There seems to be a link between the equatorial Atlantic and Benguela Niños since, in general, the anomalies in the region off the Angola and Namibia coasts occur earlier than the equatorial anomalies (not shown). *Florenchie et al.* [2004] showed that the Benguela Niño usually peaks in March/April, in contrast to the peak season (boreal summer) of the equatorial warming. It has also been suggested that subsurface temperature anomalies forced by surface wind anomalies in the west central equatorial Atlantic propagate eastward but outcrop only at regions off the Angola and Namibia coasts [e.g., *Florenchie et al.*, 2003, 2004]. However, the conclusions can be made only after further quantifying related oceanic components, particularly the variability in the subsurface ocean.

[37] 6. Finally, we have not discussed the possible impact of the NAO on the tropical Atlantic. Several past studies showed that the NAO may induce large-scale circulation anomalies and influence Caribbean rainfall through its modulation of SST in the tropical region [e.g., *Wang*, 2002; *Giannini et al.*, 2001a].

[38] **Acknowledgments.** The authors thank Chidong Zhang for commenting on an early version. We would also thank the editor, Ruth Lieberman, and three anonymous reviewers for their constructive comments and suggestions. David Bolvin prepared the GPCP rainfall data.

References

Adler, R. F., et al. (2003), The version 2 Global Precipitation Climatology Project (GPCP) monthly precipitation analysis (1979–present), *J. Hydrometeorol.*, *4*, 1147–1167.

Biasutti, M., D. S. Battisti, and E. S. Sarachik (2003), The annual cycle over the tropical Atlantic, South America, and Africa, *J. Clim.*, *16*, 2491–2508.

Biasutti, M., D. S. Battisti, and E. S. Sarachik (2004), Mechanisms controlling the annual cycle of precipitation in the tropical Atlantic sector in an atmospheric GCM, *J. Clim.*, *17*, 4708–4723.

Carton, J. A., and B. Huang (1994), Warm events in the tropical Atlantic, *J. Phys. Oceanogr.*, *24*, 888–903.

Chang, P., R. Saravanan, L. Ji, and G. C. Hegerl (2000), The effect of local sea surface temperature on atmospheric circulation over the tropical Atlantic sector, *J. Clim.*, *13*, 2195–2216.

Chiang, J. C. H., and A. H. Sobel (2002), Tropical tropospheric temperature variations caused by ENSO and their influence on the remote tropical climate, *J. Clim.*, *15*, 2616–2631.

Chiang, J. C. H., Y. Kushnir, and S. E. Zebiak (2000), Interdecadal changes in eastern Pacific ITCZ variability and its influence on the Atlantic ITCZ, *Geophys. Res. Lett.*, *27*, 3687–3690.

Chiang, J. C. H., Y. Kushnir, and A. Giannini (2002), Reconstructing Atlantic Intertropical Convergence Zone variability: Influence of the local cross-equatorial sea surface temperature gradient and remote forcing from the eastern equatorial Pacific, *J. Geophys. Res.*, *107*(D1), 4004, doi:10.1029/2000JD000307.

Curtis, S., and S. Hastenrath (1995), Forcing of anomalous sea surface temperature evolution in the tropical Atlantic during Pacific warm events, *J. Geophys. Res.*, *100*, 15,835–15,847.

Czaja, A., P. van der Vaart, and J. Marshall (2002), A diagnostic study of the role of remote forcing in tropical Atlantic variability, *J. Clim.*, *15*, 3280–3290.

Delecluse, P., J. Servain, C. Levy, K. Arpe, and L. Bengtsson (1994), On the connection between the 1984 Atlantic warm event and the 1982–1983 ENSO, *Tellus, Ser. A*, *46*, 448–464.

Deque, M., and J. Servain (1989), Teleconnections between tropical Atlantic sea surface temperatures and midlatitude 50 kPa heights during 1964–1986, *J. Clim.*, *2*, 929–944.

Enfield, D. B., and D. A. Mayer (1997), Tropical Atlantic sea surface temperature variability and its relation to El Niño–Southern Oscillation, *J. Geophys. Res.*, *102*, 929–945.

Enfield, D. B., A. M. Mestas-Nuñez, D. A. Mayer, and L. Cid-Serrano (1999), How ubiquitous is the dipole relationship in tropical Atlantic sea surface temperature?, *J. Geophys. Res.*, *104*, 7841–7848.

Florenchie, P., J. R. E. Lutjeharms, C. J. C. Reason, S. Masson, and M. Rouault (2003), The source of Benguela Niños in the South Atlantic Ocean, *Geophys. Res. Lett.*, *30*(10), 1505, doi:10.1029/2003GL017172.

Florenchie, P., C. J. C. Reason, J. R. E. Lutjeharms, M. Rouault, C. Roy, and S. Masson (2004), Evolution of interannual warm and cold events in the southeast Atlantic Ocean, *J. Clim.*, *17*, 2318–2334.

Giannini, A., M. A. Cane, and Y. Kushnir (2001a), Interdecadal changes in the ENSO teleconnection to the Caribbean region and the North Atlantic Oscillation, *J. Clim.*, *14*, 2867–2879.

Giannini, A., J. C. H. Chiang, M. A. Cane, Y. Kushnir, and R. Seager (2001b), The ENSO teleconnection to the tropical Atlantic Ocean: Con-

tributions of the remote and local SSTs to rainfall variability in the tropical Americas, *J. Clim.*, *14*, 4530–4544.
Giannini, A., R. Saravanan, and P. Chang (2004), The preconditioning role of tropical Atlantic variability in the development of the ENSO teleconnection: Implication for the predictability of Nordeste rainfall, *Clim. Dyn.*, *22*, 839–855.
Grist, J. P., and S. E. Nicholson (2001), A study of the dynamic factors influencing the rainfall variability in the West African Sahel, *J. Clim.*, *14*, 1337–1359.
Grodsky, S. A., and J. A. Carton (2003), The intertropical convergence zone in the South Atlantic and the equatorial cold tongue, *J. Clim.*, *16*, 723–733.
Gu, G., and R. F. Adler (2004), Seasonal evolution and variability associated with the West African monsoon system, *J. Clim.*, *17*, 3364–3377.
Gu, G., R. F. Adler, G. J. Huffman, and S. Curtis (2003), Summer synoptic-scale waves over West Africa observed by TRMM, *Geophys. Res. Lett.*, *30*(14), 1729, doi:10.1029/2003GL017402.
Hastenrath, S., and L. Greischar (1993), Circulation mechanisms related to northeast Brazil rainfall anomalies, *J. Geophys. Res.*, *98*, 5093–5102.
Houghton, R. W., and Y. Tourre (1992), Characteristics of low-frequency sea surface temperature fluctuations in the tropical Atlantic, *J. Clim.*, *5*, 765–771.
Janicot, S., A. Harzallah, B. Fontaine, and V. Moron (1998), West African Monsoon dynamics and eastern equatorial Atlantic and Pacific SST anomalies (1970–88), *J. Clim.*, *11*, 1874–1882.
Lamb, P. J. (1978a), Large scale tropical Atlantic surface circulation patterns during recent sub-Saharan weather anomalies, *Tellus*, *30*, 240–251.
Lamb, P. J. (1978b), Case studies of tropical Atlantic surface circulation patterns during recent sub-Saharan weather anomalies: 1967 and 1978, *Mon. Weather Rev.*, *106*, 482–491.
Landsea, C. W., R. A. Pielke Jr., A. M. Mestas-Nuñez, and J. A. Knaff (1999), Atlantic basin hurricanes: Indices of climatic changes, *Clim. Change*, *42*, 89–129.
Lanzante, J. R. (1996), Lag relationships involving tropical sea surface temperature, *J. Clim.*, *9*, 2568–2578.
Latif, M., and A. Grötzner (2000), The equatorial Atlantic oscillation and its response to ENSO, *Clim. Dyn.*, *16*, 213–218.
Liu, W. T., and X. Xie (2002), Double intertropical convergence zones: A new look using scatterometer, *Geophys. Res. Lett.*, *29*(22), 2072, doi:10.1029/2002GL015431.
Mitchell, T. P., and J. M. Wallace (1992), The annual cycle in equatorial convection and sea surface temperature, *J. Clim.*, *5*, 1140–1156.
Nobre, P., and J. Shukla (1996), Variations of sea surface temperature, wind stress, and rainfall over the tropical Atlantic and South America, *J. Clim.*, *9*, 2464–2479.
Reynolds, R. W., and T. M. Smith (1994), Improved global sea surface temperature analyses using optimum interpolation, *J. Clim.*, *7*, 929–948.
Ruiz-Barradas, A., J. A. Carton, and S. Nigam (2000), Structure of interannual-to-decadal climate variability in the tropical Atlantic sector, *J. Clim.*, *13*, 3285–3297.
Saravanan, R., and P. Chang (2000), Interaction between tropical Atlantic variability and El Niño-Southern Oscillation, *J. Clim.*, *13*, 2177–2194.
Servain, J., I. Wainer, J. P. McCreary Jr., and A. Dessier (1999), Relationship between the equatorial and meridional modes of climate variability in the tropical Atlantic, *Geophys. Res. Lett.*, *26*, 485–488.
Sutton, R. T., S. P. Jewson, and D. P. Rowell (2000), The elements of climate variability in the tropical Atlantic region, *J. Clim.*, *13*, 3261–3284.
Thorncroft, C. D., and D. P. Rowell (1998), Interannual variability of African wave activity in a general circulation model, *Int. J. Climatol.*, *18*, 1306–1323.
Uvo, C. B., C. A. Repelli, S. E. Zebiak, and Y. Kushnir (1998), The relationship between tropical Pacific and Atlantic SST and northeast Brazil monthly precipitation, *J. Clim.*, *11*, 551–562.
Wagner, R. G. (1996), Decadal-scale trends in mechanisms controlling meridional sea surface temperature gradients in the tropical Atlantic, *J. Geophys. Res.*, *101*, 16,683–16,694.
Wang, C. (2002), Atlantic climate variability and its associated atmospheric circulation cells, *J. Clim.*, *15*, 1516–1536.
Xie, S.-P., and Y. Tanimoto (1998), A pan-Atlantic decadal climate oscillation, *Geophys. Res. Lett.*, *25*, 2185–2188.
Zebiak, S. E. (1993), Air-sea interaction in the equatorial Atlantic region, *J. Clim.*, *6*, 1567–1586.

R. F. Adler and G. Gu, NASA Goddard Space Flight Center, Code 613.1, Greenbelt, MD 20771, USA. (adler@agnes.gsfc.nasa.gov; ggu@agnes.gsfc.nasa.gov)